

Mislocalization of Membrane Proteins Associated with Multidrug Resistance in Cisplatin-resistant Cancer Cell Lines¹

Xing-Jie Liang, Ding-Wu Shen, Susan Garfield, and Michael M. Gottesman²

Laboratory of Cell Biology [X.-J. L., D.-W. S., M. M. G.] and Laboratory of Experimental Carcinogenesis [S. G.], Center for Cancer Research, National Cancer Institute, National Institutes of Health, Bethesda, Maryland 20892-4254

ABSTRACT

The accumulation of [¹⁴C]carboplatin and [³H]methotrexate is reduced in single-step KB epidermoid adenocarcinoma (KB-CP) cells, which are cross-resistant to carboplatin, methotrexate, and sodium arsenite. In these KB-CP cells, multidrug resistance is accompanied by mislocalization of multidrug resistance associated protein (MRP) 1 and other membrane proteins such as folate-binding protein. MRP1 was not decreased in amount in single-step variants but accumulates in a cytoplasmic fraction, and its apparent molecular weight was altered probably because of reduced glycosylation in resistant cells. This low-density compartment was partially labeled with antibodies to lectin-GSII (a Golgi marker) and Bip/GRP78 (an endoplasmic reticulum marker). Pulse-chase labeling of MRP1 with ³⁵S-methionine and ³⁵S-cysteine and pulse-chase biotinylation of cell surface MRP1 suggests that membrane protein mislocalization is caused mainly by a defect of plasma membrane protein recycling, manifested also as a defect in acidification of lysosomes. The reduced accumulation of cytotoxic compounds in the KB-CP cells is presumed to result from the failure of carrier proteins and/or transporters to localize to the plasma membrane.

INTRODUCTION

cis-Diamminedichloroplatinum II (cisplatin) is a commonly used chemotherapeutic agent that is effective as a single agent or in combination with other drugs in the treatment of a wide variety of malignant solid tumors, including cancer of the head and neck, testes, ovaries, bladder, esophagus, as well as small cell lung cancers (1). Resistance to cisplatin represents a major obstacle to effective cancer therapy because clinically significant levels of resistance quickly emerge after treatment. Studies on cultured cells suggest that acquired cisplatin resistance is associated with defects in the apoptotic program, decreased cisplatin accumulation, and increased drug inactivation by protein and nonprotein thiols (2). Alterations of cell cycle regulators, such as cyclin D1 and c-Myc, and signal transduction pathways, such as phosphatidylinositol 3'-kinase, have also been described in association with cisplatin resistance (3, 4). However, the exact mechanisms of resistance to cisplatin require further elucidation. An improved understanding of the cellular and molecular mechanisms by which cisplatin resistance develops is necessary for cisplatin to be used most effectively.

To study cisplatin resistance in detail, we have isolated two independent cell populations derived from human KB epidermoid adenocarcinoma (KB-CP) cells and human BEL 7404 hepatoma (7404-CP) cells. These populations were derived in multiple steps by gradual increases in selecting concentration of cisplatin and share the following characteristics: (a) cross-resistance to other platinum compounds, methotrexate, heavy metals, and nucleoside analogues with no increased resistance to natural product chemotherapeutic drugs that are

known to be subject to MDR³ 1-dependent efflux (5); (b) reduced accumulation of drugs to which they are resistant, including cisplatin, carboplatin, and methotrexate (6); (c) reduced expression of cell surface proteins (1); and (d) reduced endocytosis (7).

Because this phenotype is quite complex, we sought to analyze single-step selected KB-CP variants to determine how much of this phenotype arises as a result of a single alteration in KB cells. We chose to study, in detail, the expression and subcellular distribution of two plasma membrane proteins, MRP1 and FBP, because the level of these proteins is reduced in the multistep high-level cisplatin-resistant KB cells. MRP1 is a *M_r* 190,000 integral membrane phosphoglycoprotein that belongs to the ATP-binding cassette superfamily of transport proteins, whereas FBP is a glycosylphosphatidyl inositol-linked plasma membrane protein. MRP1 is capable of conferring resistance to multiple chemotherapeutic agents, and several laboratories have reported that overexpression of MRP1 is associated with the reduction of intracellular cisplatin accumulation (8). Because previous studies from our laboratory and others showed no change or reduced, rather than increased, expression of MRP1 in CP-resistant cells (9, 10), we wished to determine expression levels and localization of this protein in the single-step variants. Similarly, FBP is reduced in high-level KB-CP variants in association with reduced uptake and cross-resistance to methotrexate, so we also determined its level of expression and localization in the single-step variants.

In the present study, we have used several independently selected single-step cisplatin-resistant variants of KB adenocarcinoma cells to explore common features related to cisplatin resistance. We investigated the effects of cisplatin resistance on MRP1 and FBP and showed mislocalization of these proteins in different variants with failure to recycle to the plasma membrane, leading to accumulation in the cytoplasm. We also demonstrate that this mislocalization of MRP1 is associated with accumulation of a partly or unglycosylated form of the protein, whereas the level of gene expression remains the same. The reduced cisplatin accumulation was associated with an intracellular redistribution of some membrane proteins including the increase of the protein in the cytoplasm. Our data indicate that the defect in single-cell variants also results in neutralization of the acidic pH of lysosomes, suggesting a general defect in regulation of endocytosis and membrane vesicle recycling. We conclude that this pleiotropic defect results in reduced cell surface expression of proteins [MRP1, FBP, as well as a hypothetical cisplatin-binding protein(s)] that are essential for uptake of cisplatin and other toxic compounds such as folate antagonists, heavy metals, and nucleoside analogues.

MATERIALS AND METHODS

Isolation and Maintenance of Cisplatin-resistant Cells. KB-3-1, the parent cell line for the drug-resistant variants described in this study, was derived from a single clone of human KB epidermoid carcinoma cells (a variant of HeLa) after two subclonings from the parental cells (11). The cisplatin-resistant sublines were selected in a single exposure to cisplatin at 0.3

Received 2/12/03; revised 6/13/03; accepted 7/1/03.

The costs of publication of this article were defrayed in part by the payment of page charges. This article must therefore be hereby marked *advertisement* in accordance with 18 U.S.C. Section 1734 solely to indicate this fact.

¹ Supported by the National Institutes of Health.

² To whom requests for reprints should be addressed, at Laboratory of Cell Biology, Building 37, Room 1A09, National Cancer Institute, National Institutes of Health, 37 Convent Drive MSC 4254, Bethesda, MD 20892-4254. Phone: (301) 496-1530; Fax: (301) 402-0450; E-mail: mgottesman@nih.gov.

³ The abbreviations used are: MDR, multidrug resistance; MRP, MDR associated protein; FBP, folate-binding protein; mAb, monoclonal antibody; EGF, epidermal growth factor; Ca/Mg-PBS, calcium- and magnesium-supplemented PBS; RIPA, radioimmuno-precipitation assay; ER, endoplasmic reticulum; CP, cisplatin.

$\mu\text{g/ml}$ (KB-CP.3) or at $0.5 \mu\text{g/ml}$ (KB-CP.5). 1×10^6 cells were plated in 100-mm dishes in the indicated concentration of cisplatin. Clones began to appear after 12 days at a frequency of 150 per 10^6 cells in $0.3 \mu\text{g/ml}$ cisplatin and 60 per 10^6 cells in $0.5 \mu\text{g/ml}$ cisplatin. Medium containing cisplatin was changed every 4 days, and small (S), medium (M), and large (L) clones were picked after 30 days and propagated in the selecting concentration of cisplatin. For the second-step variant, KB-CP1, clone KB-CP.3 (M1), was expanded, and 1×10^6 cells were plated in 100-mm dishes at $1 \mu\text{g/ml}$ cisplatin. Clones appeared after 15 days at a frequency of 80 per 10^6 cells and were picked after 26 days and grown in $1 \mu\text{g/ml}$ cisplatin. KB-CP20 was a population of KB-3-1 cells grown in increasing concentrations of cisplatin up to $20 \mu\text{g/ml}$ cisplatin over a period of 6 months. KB-CP20 was maintained in medium containing $5 \mu\text{g/ml}$ cisplatin for these experiments (12). Clones KB-CP.3 (M1), KB-CP.5 (M2), and KB-CP1 (S2) were used for the experiments described here.

The cell lines were all grown as monolayer cultures at 37°C in 5% CO_2 using DMEM with 10% premium FCS (lot 0S010F; BioWhittaker Inc., CAMBREX Bioproducts, Walkersville, MD), L-glutamine, penicillin (50 units/mol), and streptomycin (50 $\mu\text{g/ml}$; Quality Biological Inc., Gaithersburg, MD).

Drugs and Chemicals. [^{14}C]carboplatin and [^3H]methotrexate (specific activity, 20 $\mu\text{Ci/mmol}$) were purchased from Amersham Pharmacia Biotech Products (Piscataway, NJ). mAb MRP1 against human MRP1 was obtained from Alexis Biochemicals Co. (San Diego, CA). Anti-FBP antibody was obtained from Biogenesis Ltd. (Poole, United Kingdom). Anti-EGF receptor antibody EEA1 and Bip/GRP78 were obtained from Transduction Laboratories (Lexington, KY). LysoSensor DND-189 and Alexa Fluor 594-conjugated lectin-GSII were obtained from Molecular Probes (Eugene, OR). Cisplatin, methotrexate, sodium arsenate, 5-fluorouracil, and *Pseudomonas* exotoxin were from Sigma Products (St. Louis, MO).

Drug Sensitivity Assay. Dose-response curves of the human tumor cell lines were determined as described previously (1). Three to five colonies were expanded in the selecting concentration of cisplatin and tested for their resistance to cisplatin, carboplatin, methotrexate, sodium arsenite, 5-fluorouracil, and *Pseudomonas* exotoxin. Briefly, 5×10^4 cells in 1 ml of medium were inoculated into each well of a 24-well dish. At the time of seeding, the respective drugs at desired concentrations were introduced into the cell medium. After incubation for 3 days at 37°C , cells were counted with a Coulter counter. IC_{50} was measured as the concentration of drug reducing the growth of cells to 50% of that in control (drug-free) medium. A relative resistance factor for each drug was determined by dividing the IC_{50} value of the drug for the cisplatin-resistant cell lines by that for the appropriate parental cell line, KB-3-1. The values are means of triplicate determinations.

Measurement of Uptake of [^{14}C]Carboplatin and [^3H]Methotrexate. Cells were seeded 48 h before assay at 1×10^5 cells/ml of medium without cisplatin per well in each well of a 24-well culture dish (Costar, Corning, NY). Cells were washed once with prewarmed regular DMEM. [^{14}C]carboplatin (1 μCi) was added or [^3H]methotrexate (0.5 μCi) was added in 0.3 ml of medium per well of cells. Cells were reincubated immediately at 37°C for 1 h. To terminate the incubation, cells were washed with ice-cold PBS three times, then harvested by trypsinization. The cell suspensions in 200 μl of PBS were transferred from each well into counting vials with scintillation mixture (Formula 989; DuPont NEN, Boston, MA). The radioactivity of the sample was measured in a Beckman LS3801 liquid scintillation counter (Fullerton, CA). Duplicates were made from each well for cell counting at the same time.

Immunoblotting Detection of MRP1 Protein. 1×10^7 cells from each cell line grown without cisplatin for at least 3 days were harvested at log phase and washed twice with cold PBS. The cells were sedimented by centrifugation at $1,400 \times g$ for 10 min and suspended in ice-cold hypotonic solution buffer [0.5 mM KH_2PO_4 and 0.1 mM EDTA containing 1% protease inhibitor aprotinin (pH 8.0)] for 5 min on ice. Cells were disrupted on ice by a tight Dounce homogenizer with constant homogenizing for 30 strokes. Samples were checked under a phase-contrast microscope and showed more than 80% of cells broken. The cytosol fractions were separated by centrifugation at $2,000 \times g$ for 10 min at 4°C . The resulting low-speed supernatant was further centrifuged at $100,000 \times g$ (equal to 45,000 rpm in an RP45-A rotor for the Sorvall centrifuge) for 55 min at 4°C . The membranes sedimenting at the bottom (membrane fraction) were collected, as was the $100,000 \times g$ supernatant (cytosol fraction). The membranes were dissolved directly into 5% SDS buffer and stored at -80°C until use. Protein electrophoresis and immunoblotting with antibodies directed to MRP1 were performed as described pre-

viously (10). Briefly, the samples (plasma membrane-enriched fraction and cytosolic fraction) were separated by SDS-PAGE on a 4–20% gradient gel and transferred onto nitrocellulose membranes. Subsequently, membranes were subjected to immunostaining with mAbs against human MRP1 (1:2000, 1 h at room temperature). Enhanced chemiluminescence reagents were used for developing signals as described by the manufacturer (Pierce Chemical Co., Rockford, IL).

Indirect Immunofluorescence Microscopy. The cells cultured on 18-mm glass coverslips in medium without cisplatin were fixed at 4°C with 3.5% formaldehyde (EM grade; Polysciences, Inc., Warrington, PA) in PBS for 10 min. Subsequently, cells were washed with PBS and incubated with 0.1% Triton X-100 in PBS for permeabilization. Cells were preblocked in 3% BSA/PBS for 30 min, then incubated for 1 h with primary antibodies against MRP1 (rat monoclonal, diluted 1:40; Alexis Biochemicals, Carlsbad, CA), FBP (mouse monoclonal, 1:35; Biogenesis Ltd.), and the ER marker protein (Bip/GRP78, 1:25; Transduction Laboratories) or Golgi marker protein (Alexa Fluor 549-conjugated lectin-GSII), which was followed by a 1-h incubation with rhodamine- or FITC-labeled secondary antibodies (1:50; Jackson ImmunoResearch Laboratories) before mounting on slides with fluorescence mounting medium (DAKO Corp., Carpinteria, CA). Controls with nonimmune IgG and secondary antibody alone were negative. For colocalization experiments, MRP1 was combined with Bip or lectin (Molecular Probes, Inc.). Background fluorescence was determined by applying the secondary antibody alone, a FITC-conjugated, affinity-purified goat antirat IgG. Confocal fluorescent images were collected with a Bio-Rad (Hercules, CA) MRC 1024 confocal scan head mounted on a Nikon Optiphot microscope with a $\times 60$ planapochromat lens. Excitation at 488 nm and 568 nm was provided by a krypton-argon gas laser. Emission filters of 598/40 and 522/32 were used for collecting red and green fluorescence, respectively, in channels one and two, whereas phase contrast images of the same cell were collected in the third channel using a transmitted light detector. After sequential excitation, red and green fluorescent images of the same cell were merged for colocalization using LaserSharp software (Bio-Rad).

Iodixanol Equilibrium Gradient Centrifugation. The low-speed supernatant fraction without nuclei prepared from KB-3-1 and KB-CP.5 cells, as described above, was suspended in homogenization buffer [0.25 M sucrose, 1 mM EDTA, and 10 mM HEPES-NaOH (pH 7.4)]. The iodixanol (Optiprep) was mixed with homogenization buffer to a 25% final concentration. The supernatant fraction was layered on top of the gradient. A self-generating gradient was formed in a 3.0 ml unsealed tube (Hitachi Koki Co., Ltd., Hitachinaka, Japan) by centrifuging to equilibrium at 4°C with a S100 vertical rotor (Sorvall) at 365,000 for 60 min. Fractions (~ 0.3 ml) were collected by upward displacement from the top of the tube and analyzed by immunoblotting. The density of each fraction was determined by weighing an aliquot, and gradients used to analyze KB-3-1 and KB-CP.5 cells were found to be the same.

^{35}S -Methionine, ^{35}S -Cysteine Metabolic Labeling, Pulse-Chase Analysis, and Immunoprecipitation. KB-3-1 and KB-CP.5 cells growing in log phase were used for pulse-chase experiments. Fresh media with FBS were added 6 h before cells were deprived of methionine for 30 min. Cells were labeled for 15 min with 2 ml of methionine-free and cysteine-free DMEM from Life Technologies, Inc., Invitrogen Corp. (Grand Island, NY) containing 29.6 MBq (800 μCi) ^{35}S Protein Labeling Mix (50% L- ^{35}S -methionine and 50% L- ^{35}S -cysteine; Amersham Pharmacia Biotech Products) in a 5% CO_2 incubator at 37°C . A chase was then performed in 4 ml of DMEM medium containing unlabeled L-methionine (30 mg/liter; Life Technologies, Inc., Invitrogen Corp.) for various time periods. At each time point, cells were harvested and prepared in 200 μl of ice-cold hypotonic solution as mentioned above.

Homogenizations were performed using a 2-ml Dounce homogenizer fitted with a tight pestle. Homogenates were centrifuged at $2,000 \times g$ for 10 min to discard all nuclei and spun at $25,000 \times g$ (23,000 rpm for the RP45-A rotor) for 25 min to pellet all other organelles, then at $100,000 \times g$ (45,000 rpm for the RP45-A rotor) for 55 min to collect the cellular membranes and the cytosol-containing supernatant. The pellet of the high-speed fraction was dissolved in 100 μl of RIPA buffer (20 mM Tris-HCl, 0.15 M NaCl, 0.5% Triton X-100, 0.05% SDS, and 1% aprotinin).

Immunoprecipitation of MRP1 was accomplished by incubating prepared cell lysates and conditioned media with 2 μg of mAb MRP1 for 2 h at 4°C . The resulting immune complexes were adsorbed with 20 μl of 20% (vol/vol) protein G-Sepharose (Santa Cruz Biotechnology, Santa Cruz, CA). Pellets

were washed four times in RIPA assay buffer, resuspended either in buffer for further trichloroacetic acid precipitation or in PAGE sample buffer. The immunoprecipitated proteins were resolved by SDS-PAGE in 4–20% (wt/vol) gels, and the radioactivity incorporated into MRP1 bands was analyzed using radiography on BIOMAX-MR film (Eastman-Kodak Co., Rochester, NY).

Cell Surface Biotinylation and Immunoprecipitation. The cells were grown in a T75 flask to 90% confluence in medium without cisplatin and incubated in fresh media without methionine for 4 h. Then, the cells were washed three times with Ca/Mg-PBS (pH 8.1). Sulfo-NHS-LC-biotin (Pierce Chemical Co.) solution (5 mg/ml) in Ca/Mg-PBS was incubated with cells for 30 min at 4°C with agitation (sulfo-NHS-LC-biotin; Pierce Chemical Co.). Free sulfo-NHS-biotin was removed by washing five times with ice-cold Ca/Mg-PBS. Biotinylated cells were treated as described previously to isolate the membrane pellet and supernatant. The membrane pellet was solubilized in 0.5 ml of RIPA assay buffer as mentioned above, supplemented with 1% protease inhibitor with gentle shaking. To 500 µl of each supernatant were added 5 µl of the MRP1 mAb, which is directed against the MRP1 protein. After agitation for 4 h at 4°C, 30 µl of a 50% slurry of protein G-Sepharose was added; the immunoprecipitates were collected by centrifugation (16,000 × g for 3 min), washed three times with NP40 lysis buffer, and eluted by boiling the beads in 2-fold-concentrated SDS sample buffer. The immunoprecipitates were electrophoresed on a SDS-10% polyacrylamide gel under reducing conditions and transferred to nitrocellulose by the semidry blotting technique. The membrane was incubated with blocking reagent overnight at 4°C, washed three times with PBS containing 0.1% Tween 20, and incubated with streptavidin-peroxidase for 1 h at room temperature. The nitrocellulose was washed as described previously and incubated for 1 min with a chemiluminescent peroxidase substrate. The resulting blot was visualized by short-term exposure of the membrane to Biomax autoradiography film (Eastman-Kodak).

Lysosomes Labeled by LysoTracker and LysoSensor. For adherent parental KB and KB-CP cells, cells were grown for 3 days on coverslips inside a Petri dish containing DMEM without cisplatin. When cells reached 80% confluence, the medium was removed from the dish, and the prewarmed probe-containing medium was added. The final concentration was 100 nM for LysoTracker (Molecular Probes) red DND-99 and 1.5 µM for the LysoSensor (Molecular Probes) green DND-189 probe. Cells were then incubated for 30 min in 5% CO₂ at 37°C. Before observation by confocal microscopy, the loading solution was replaced with fresh DMEM medium.

RESULTS

Cross-Resistance to Cytotoxic Drugs of Single-Step Cisplatin-resistant Cells. Drug sensitivity assays were performed as described in “Materials and Methods.” The relative resistance level for KB-CP.3 isolated in 0.3 µg/ml cisplatin was 4-fold higher than the parental KB-3-1 cells. The single-step cisplatin-resistant cell line KB-CP.5 and the two-step variant KB-CP1 (derived in a second step from KB-CP.3) were 40- and 90-fold more resistant to cisplatin than their parental cell

line, respectively. To determine the cross-resistance patterns in both parental and resistant KB cell lines, several agents were examined as shown in Table 1. A total of 12 clones that survived cisplatin exposure were propagated in the selecting concentration of cisplatin and tested for resistance to the cytotoxic agents. The KB-CP cells showed high levels of resistance to cisplatin, carboplatin, methotrexate, and sodium arsenite. Little or no cross-resistance to *Pseudomonas* exotoxin and 5-fluorouracil, seen in multistep KB-CP variants, was detected in single-step KB-CP cells, but the second-step KB-CP1 cells showed low cross-resistance to these cytotoxic agents.

Reduced Accumulation of [¹⁴C]Carboplatin and [³H]Methotrexate in Cisplatin-resistant Cells. Accumulation of [¹⁴C]carboplatin and [³H]methotrexate was determined as described in “Materials and Methods” for the parental KB cells and the single-step CP variants. Cells were incubated with 1 µCi of [¹⁴C]carboplatin or 0.5 µCi of [³H]methotrexate at 37°C for 1 h, after which the radioactivity retained in the cells was measured. The results are shown in Fig. 1, A and B, respectively. Fig. 1 shows a reduction of [¹⁴C]carboplatin and [³H]methotrexate accumulation at 37°C in proportion to the extent of CP resistance compared with the parental KB-3-1 cell line.

Immunoblotting to Localize MRP1. Because altered MRP1 expression has been observed in other cell lines with cisplatin resistance (8), we sought to determine the levels of MRP1 in KB-CP cells. Fig. 2 shows an immunoblot analysis to determine levels of MRP1 using mAb MRPr1 directed to human MRP1 with visualization by enhanced luminol reagent. Enriched membrane proteins were isolated from each cell line as described in “Materials and Methods.” The cisplatin-sensitive parental cell line KB-3-1 expresses abundant MRP1 in membrane-enriched preparations, whereas the presence of MRP1 was decreased in the membrane (pellet) fraction and increased in the high-speed supernatant (cytosolic) fraction in the cisplatin-resistant cell lines. The apparent molecular weight of MRP1 was reduced in the CP-resistant single-step KB cells; at high levels of resistance (KB-CP20), this reduction was even more pronounced. This reduction in molecular weight appeared to be caused by reduced glycosylation, because it could be mimicked by treating KB-3-1 membrane preparations with *N*-endoglycosidase (data not shown). The expression of the MRP1 mRNA was similar between the cisplatin-sensitive and cisplatin-resistant single-step KB-CP cells as determined by semi-quantitative RT-PCR (data not shown).

Immunofluorescence to Localize MRP1 and FBP. Indirect immunofluorescence localization of MRP1 demonstrates that MRP1 is strongly expressed at the plasma membrane in the cisplatin-sensitive KB-3-1 cells (Fig. 3A, top left). However, in KB-CP cells, localization within the cytoplasm is seen clearly (Fig. 3A). The mislocalization of

Table 1 Patterns of cross-resistance in parental and cisplatin-resistant human KB epidermoid carcinoma cell lines

Chemicals Clone designation	KB	KB-CP.3 ^a (LD ₅₀ , µg/ml)				KB-CP.5 ^b (LD ₅₀ , µg/ml)					KB-CP1 ^c (LD ₅₀ , µg/ml)		
		S5	L1	M1	M3	M1	M2	L6	L4	L2	S2	M2	L6
Cisplatin	0.064	0.25	0.16	0.27	0.5	2.8	3.2	2.9	1.9	1.5	6.4	5.7	7.1
Relative resistance ^d		4	2.6	4.4	8	44	50	45	30	23	100	89	110
Carboplatin	0.7	7	3.5	5	10	15	24	16	20	13	40	32	38
Relative resistance		10	5	7	14	21	34	22	29	18	57	45	54
Methotrexate	0.0032	0.01	0.005	0.004	0.01	0.018	0.024	0.007	0.004	0.01	0.025	0.022	0.034
Relative resistance		3.1	1.5	1.25	3.1	5.6	7.4	2.1	1.3	3.1	7.8	6.8	10.6
Sodium arsenite	0.31	0.39	0.32	0.32	0.64	1.3	1.6	0.47	0.58	0.7	2.8	2.5	3.3
Relative resistance		1.3	1	1	2.1	4	5.2	1.5	1.9	2.3	9	8.1	10.6
5-Fluorouracil	0.36	0.40	0.34	0.38	0.41	0.45	0.6	0.41	0.46	0.6	0.84	0.74	0.82
Relative resistance		1.1	1	1	1.1	1.3	1.7	1.1	1.3	1.7	2.3	2	2.3
<i>Pseudomonas</i> exotoxin	0.015	0.017	0.014	0.016	0.016	0.017	0.018	0.020	0.014	0.018	0.026	0.022	0.028
Relative resistance		1.1	1	1	1	1.1	1.2	1.4	1	1.2	1.7	1.5	1.9

^a Maintained in medium containing 0.3 µg/ml⁻¹ cisplatin.

^b Maintained in medium containing 0.5 µg/ml⁻¹ cisplatin.

^c Maintained in medium containing 1 µg/ml⁻¹ cisplatin.

^d Relative resistance was determined by dividing the LD₅₀ value (µg/ml⁻¹) of the drug for cisplatin-resistant KB cells by that for the parental KB-3-1 cell line.

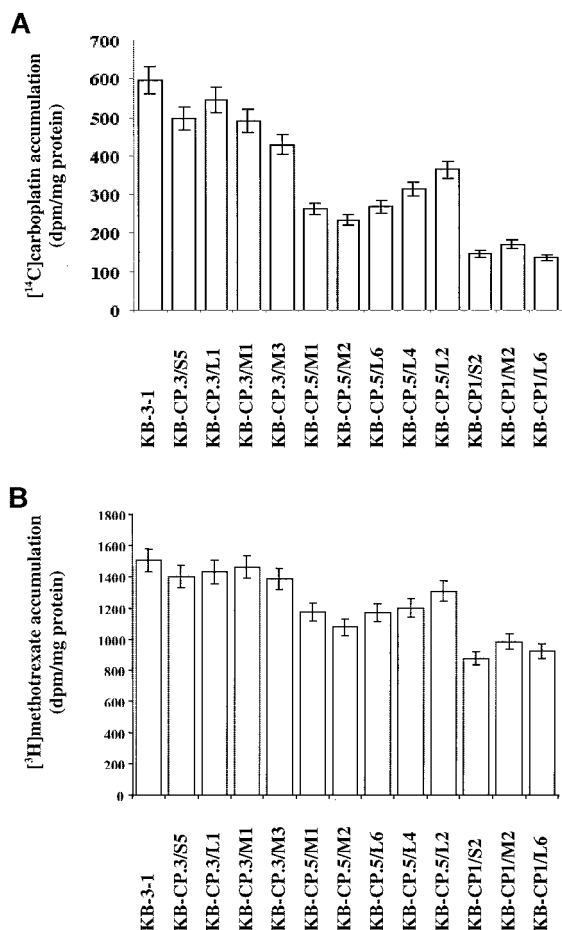


Fig. 1. Accumulation of [¹⁴C]carboplatin and [³H]methotrexate in CP-sensitive and single-step CP-resistant colonies. Cells were seeded at 10⁵ cells/ml of medium per well in a 24-well cell culture dish 24 h before assays. Cells were washed once with prewarmed DMEM. A, [¹⁴C]carboplatin (1 μCi) was added in 0.3 ml of medium per well. Cells were reincubated immediately at 37°C for 1 h. To terminate the incubation, cells were washed with ice-cold PBS three times, then harvested by trypsinization and suspended in 200 μl of PBS. The cell suspensions were transferred from each well into counting vials with Formula 989. The error bars show the range of the triplicate values. B, [³H]methotrexate (0.5 μCi) was added in 0.3 ml of medium per well, then treated as described for A. A *t* test was used for statistical analysis to demonstrate reduced uptake in the resistant cells.

FBP is similar to that of MRP1 in the CP-sensitive and CP-resistant KB cells (Fig. 3B), except that FBP appears to have a more Golgi-like distribution in KB-CP cells than MRP1. As a control, EGF receptor is expressed on the cell surface in both KB and KB-CP cells (Fig. 3C).

CP-sensitive and CP-resistant KB cells were also costained with antibodies to MRP1 and GSII-lectin or Bip/GRP78. The GSII-lectin recognizes nonreducing α- or β-linked *N*-acetyl-D-glycosamine residues and is a highly selective fluorescence marker specific for the Golgi apparatus in cells (13). Bip/GRP78 is the major chaperone of the ER, which can bind nascent proteins entering the lumen. From the costaining results shown in Fig. 4, we conclude that MRP1 may be partially localized with the Golgi, and to some extent with the ER, in the CP-resistant KB cells. However, the appearance of the *trans*-Golgi network in these experiments is somewhat altered in the resistant cells, and this affects our ability to precisely localize MRP1.

Iodixanol Equilibrium Sedimentation Analysis of MRP1. To further characterize the intracellular compartment in which MRP1 is localized in KB-CP cells, we used iodixanol in an equilibrium centrifugation analysis to segregate the crude MRP1 vesicle fraction obtained from KB-3-1 and KB-CP.5 cells. The reproducible density of each fraction was confirmed by direct measurement of density as weight of fraction per volume. MRP1 was enriched in lighter fractions

in KB-CP.5 cells than in KB-3-1 cells (Fig. 5). LAMP-1, a lysosomal membrane marker that recycles to the plasma membrane, and GM130, a marker of the *cis*-compartment of the Golgi apparatus, were also found predominantly in this light membrane fraction in the KB-CP.5 cells, suggesting that these proteins may also colocalize in the same population of vesicles as MRP1, consistent with immunoelectron microscopic experiments (data not shown). We reproducibly find that whereas membrane proteins such as MRP1 and LAMP-1 are resolved into distinct peaks by iodixanol density gradient analysis, other proteins, such as Bip/GRP78, are not as well resolved, presumably because they were found in vesicles of various densities that are separated by these very shallow gradients. These density gradient data are consistent with the accumulation of MRP1, LAMP-1, and GM130 in a low-density compartment in KB-CP.5 cells.

Pulse-Chase Labeling of MRP1 with ³⁵S-Methionine and ³⁵S-Cysteine. We wished to determine whether the reduced amount of MRP1 on the cell surface resulted from failure of MRP1 to get to the cell surface or failure to stay on the cell surface. A pulse-chase protocol was used to label metabolically recently synthesized MRP1 and follow its appearance. KB parental and KB-CP.5 cells were labeled metabolically with ³⁵S-methionine and ³⁵S-cysteine. MRP1 was immunoprecipitated from the cell lysates with mAb MRP1. Fig. 6A shows autoradiographs of immunoprecipitates separated by Tricine-SDS-PAGE under reducing conditions. The two left panels indicate pulse-chase labeling of MRP1 in membrane fractions. As can be seen, for both KB and KB-CP.5 cells, ³⁵S-labeled MRP1 appears during the 15-min pulse period in the membrane pellet. For KB cells, MRP1 remains at relatively the same levels in the membrane fraction, but for KB-CP.5 cells, there is a 4-fold reduction in membrane-associated MRP1 during the 6-h chase. The differences between KB and KB-CP cells are even more obvious when labeled MRP1 was compared during the chase in the cytosol fractions. Whereas there is little or no MRP1 in the cytoplasmic fraction in KB cells, the majority of MRP1 accumulates over time in the cytoplasmic fraction in KB-CP.5 cells. We interpret this result to indicate that MRP1 in KB-CP cells can get to the plasma membrane, but that once it leaves it cannot recycle back.

Surface Labeling of KB-CP Cells with Sulfo-NHS-LC-Biotin. To confirm the hypothesis that KB-CP cells have a defect in recycling MRP1 from the cell surface, we measured MRP1 transport from the cell surface to the cytosol using pulse-chase labeling with biotin of

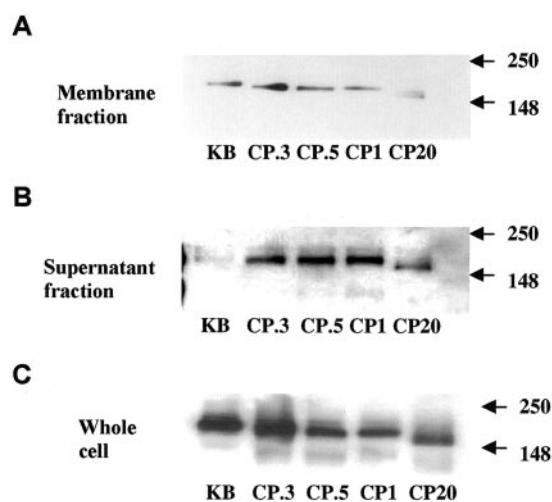


Fig. 2. Western blot of MRP1 in membrane and cytosol fractions in KB parental and KB-CP-resistant cells. A, MRP1 expression in the membrane fraction of KB parental and KB-CP-resistant cells. B, MRP1 expression in the cytosol fraction. C, MRP1 in the whole cell lysate.

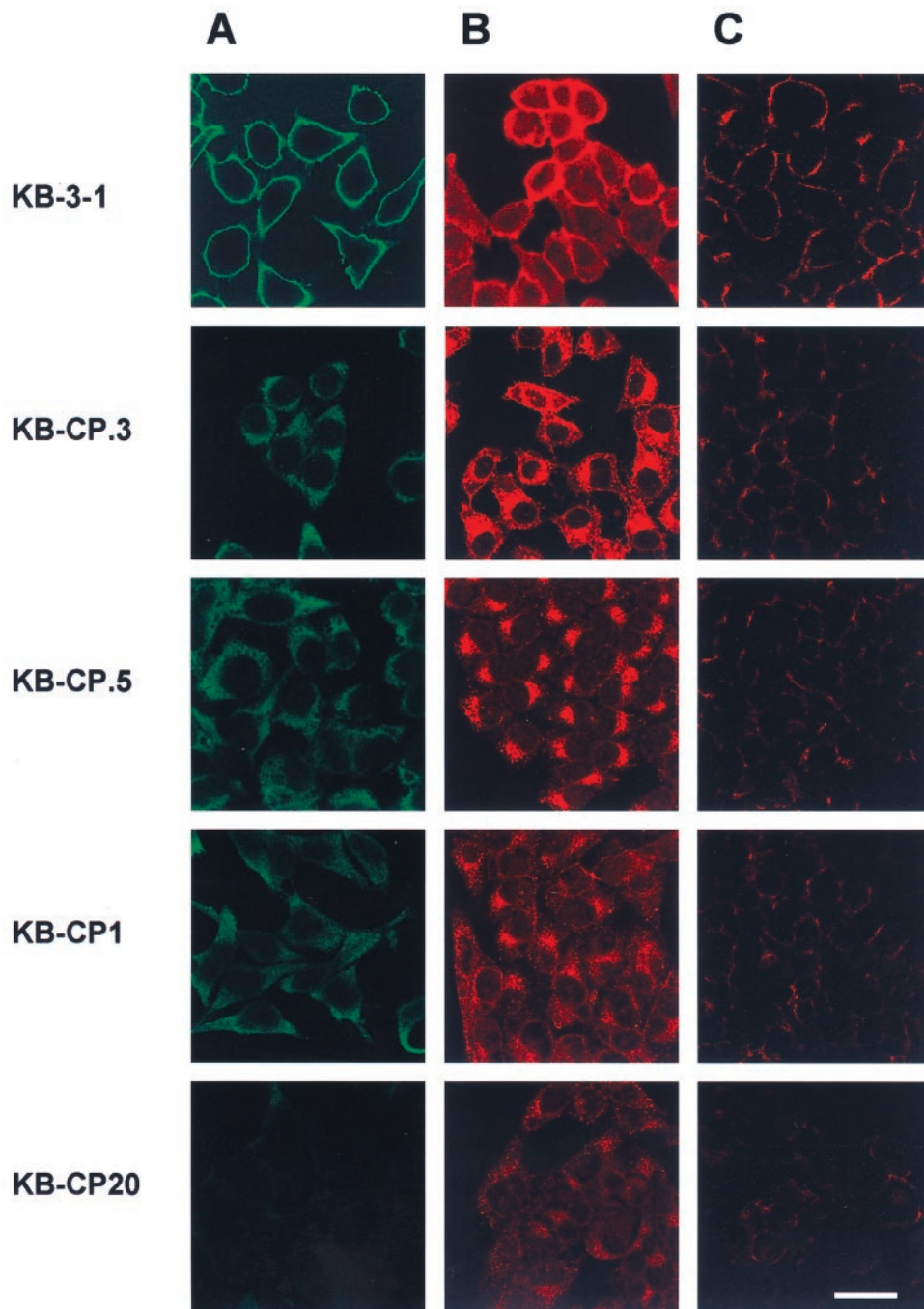


Fig. 3. Indirect immunofluorescence to localize MRP1 (A), FBP (B), and EGF receptor (C) in CP-sensitive and CP-resistant KB cells. A, cells were plated on 18-mm coverslips at 1×10^5 cells cm^{-2} after growth without cisplatin for 3 days. Cells were excited at 488 nm as indicated, and fluorescence emission at 520 nm was recorded by confocal fluorescence microscopy. A confocal optical section is shown midway through a typical sphere. MRP1 was detected by indirect immunofluorescence, as described in "Materials and Methods." B, indirect immunofluorescence of FBP. Excitation was at 590 nm, as indicated, and emission was at 615 nm. FBPs are stained with an anti-FBP antibody, as described in "Materials and Methods." C, EGF receptors are stained as in B. Scale bar, 10 μm .

cell surface MRP1. Surface proteins of KB cells were labeled with sulfo-NHS-LC-biotin at 4°C for 30 min. After incubation at 37°C in medium without the biotin label for varying times, cells were lysed as described in "Materials and Methods," and MRP1 was immunoprecipitated. Fig. 6B shows an autofluorograph of immunoprecipitates separated by 4–20% SDS-PAGE gel electrophoresis. As seen in the two left panels of Fig. 6B, MRP1 is labeled on the cell surface in both KB and KB-CP cells, although intensity of labeling is reduced in the KB-CP.5 cells. The membrane-associated MRP1 label remains high on the KB cell surface but disappears from the KB-CP.5 surface during the 18-h chase. In the two right panels of Fig. 6B, cytosol fractions indicate transient biotinylated MRP1 in KB cells, but biotinylated MRP1 accumulated in the cytosol of KB-CP.5 cells. These results are interpreted as showing recycling of cell surface MRP1 in the KB cells and little or no recycling of MRP1 in the KB-CP.5 cells.

Neutralization of Lysosomes Labeled by LysoSensor Green DND-189. To begin to determine the reason for the recycling defect in KB-CP cells, we looked at the pH of intracellular vesicles. It is well known that vesicle recycling is sensitive to the intracellular compartment pH (14). We began by measuring lysosome pH by labeling the living cells for 15 min with 1.5 μM LysoSensor green DND-189, which is an acidotropic probe with a pH-dependent increase in fluorescence intensity on acidification. It shows strong fluorescence intensity in acidic organelles. As seen in Fig. 7A, the lysosomes are alkalinized in the KB-CP cells as indicated by the decreased number and intensity of fluorescently labeled lysosomes, and alkalinization is increased in proportion to the extent of CP resistance. At the same time, the presence of lysosomes is confirmed by labeling with LysoTracker red DND-99, which exhibits fluorescence that is largely

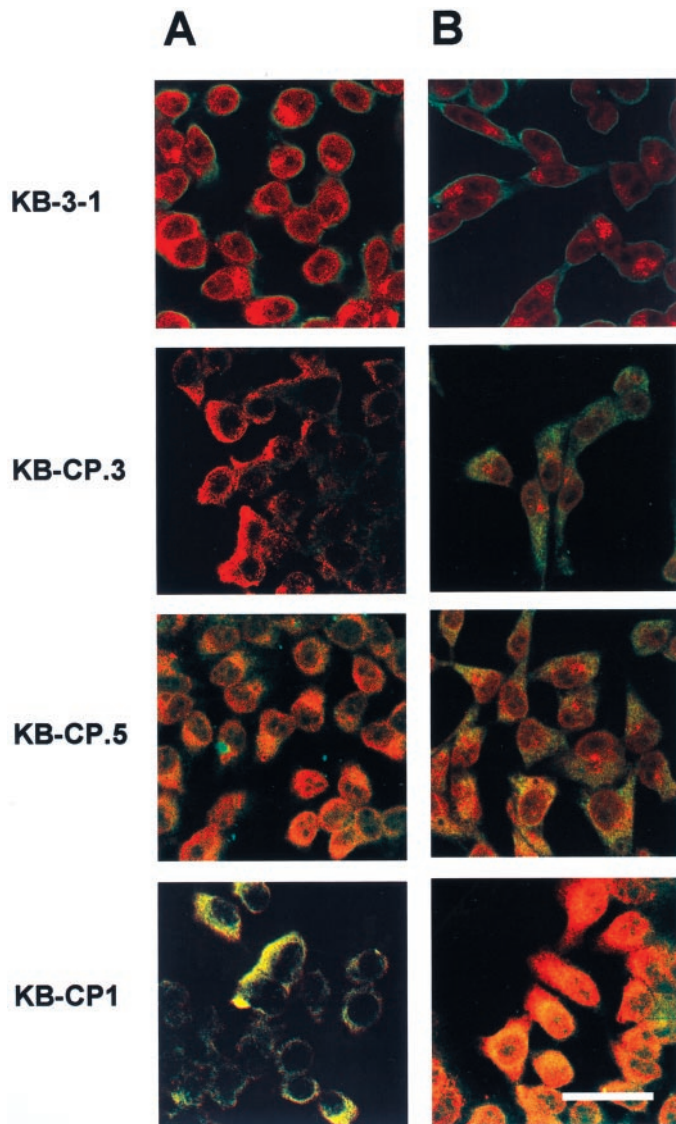


Fig. 4. Fluorescence colocalization of MRP1, ER, and Golgi in CP-sensitive and CP-resistant KB cells. *A*, cells were plated on 18-mm coverslips at 1×10^5 cells cm^{-2} after growth without cisplatin for 3 days. Cells were excited at 488/590 nm as indicated, and fluorescence emission at 508/615 nm was recorded by fluorescence microscopy. A confocal optical section is shown midway through a typical sphere. MRP1 is stained with an anti-MRP1 antibody, which is shown in *green* by a FITC-conjugated antirat second antibody IgG. The ER is stained with a marker protein antibody, Bip/GRP 78, which is shown in *red* by a rhodamine (tetramethylrhodamine isothiocyanate)-conjugated anti-mouse second antibody IgG. *B*, Golgi is stained with an Alexa Fluor 594-conjugated Lectin fluorescence probe, which stains selectively the Golgi apparatus within cells. Scale bar, 20 μm .

independent of pH. Fig. 7B shows that the number and morphology of lysosomes are similar in the parental KB cells and KB-CP cells.

DISCUSSION

Cisplatin is an important chemotherapeutic drug used to treat solid cancers. In this work, we have studied the mechanism of resistance to cisplatin in KB cells, a cultured human epidermoid carcinoma cell line. Previous work from our laboratory using this cell line has focused on cells selected in many steps to high levels of resistance in which decreased accumulation of cisplatin is associated with cross-resistance to other anticancer drugs and heavy metals (12). A similar phenotype was found in a human hepatoma cell line similarly selected in multiple steps to high levels of resistance (6). To determine whether

the complex phenotype resulted from many different cellular alterations occurring during the multistep selection, we isolated single-step variants and have now shown that, even in a single-step, it is possible to observe cross-resistance to methotrexate and heavy metals associated with decreased accumulation of carboplatin and methotrexate. Furthermore, this phenotype is accompanied by a mislocalization of at least two membrane proteins, MRP1 and FBP.

Detailed analysis of MRP1 subcellular localization suggests that the defect results from a failure to recycle MRP1 from a membrane compartment so that MRP1 accumulates in a low-density cytoplasmic, vesicular compartment in the cisplatin-resistant cells. We hypothesize that the cross-resistance pattern reflects this general cellular defect in that the cytotoxic molecules to which resistance occurs are normally brought into the cells via cell surface carriers, transporters, and/or channels that are reduced in amount on the cell surface of the resistant cells because of a decreased ability of these proteins to recycle back to the cell surface. For cisplatin, these carriers, transporters, and/or channels are not yet known, but recent reports suggest a possible contribution of copper transporters (15).

Where does MRP1 accumulate in the resistant cells? Using a variety of experimental approaches, including confocal fluorescence

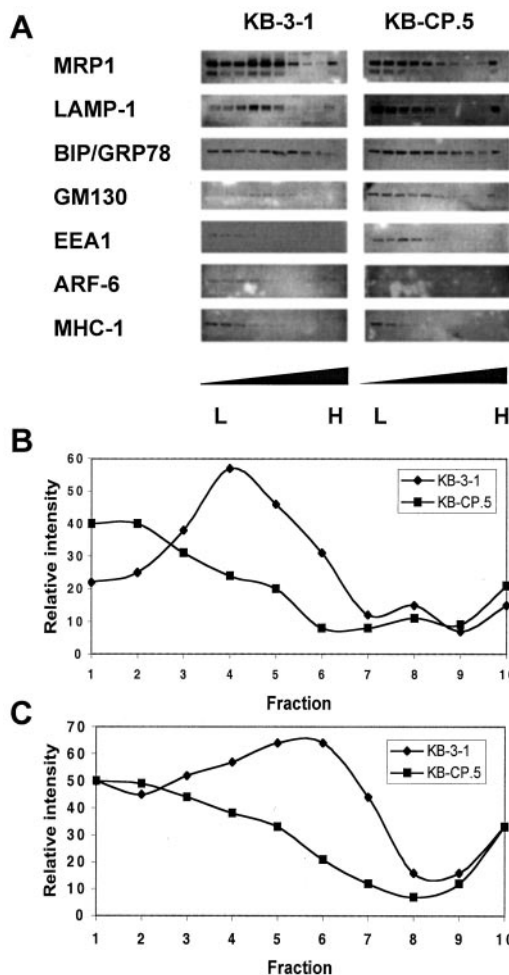


Fig. 5. Iodixanol equilibrium gradient sedimentation analysis of MRP1. *A*, the low-speed supernatant fraction prepared from KB-3-1 and KB-CP.5 cells without nuclei was subjected to iodixanol density gradient analysis, as described in "Materials and Methods." Fractions were collected from the top of the gradient and used to measure protein concentration or the distribution of various proteins by immunoblotting for KB-3-1 and KB-CP.5 cells. The results shown are from a single iodixanol gradient analysis and are representative of three experiments. *B*, MRP1 distribution in different fractions after iodixanol gradient centrifuge. Data were from a digital analysis of Western blotting with α Imager software. *C*, LAMP-1 distribution, measured as in *B*.

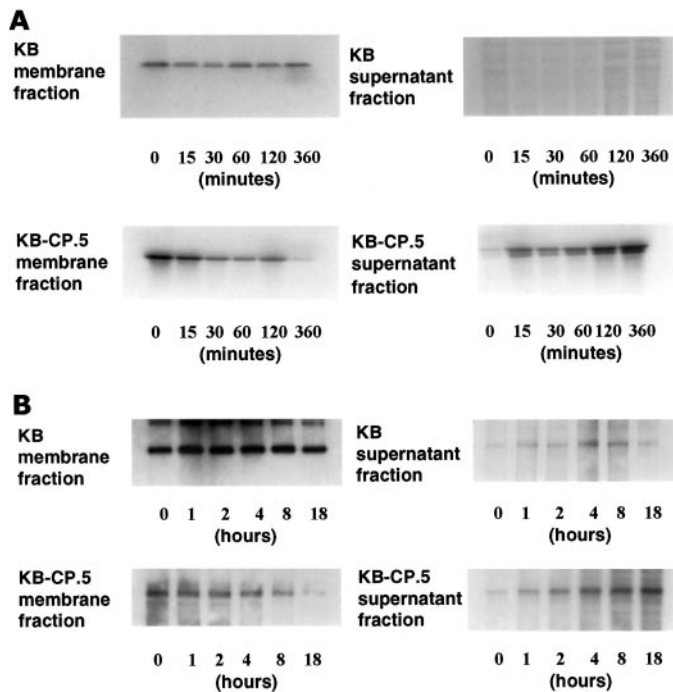


Fig. 6. Pulse-chase metabolic and cell surface labeling of MRP1. A, cell proteins were labeled with ³⁵S-methionine and ³⁵S-cysteine for 15 min and chased for the time shown. MRP1 was immunoprecipitated, as described in "Materials and Methods," from membrane pellets and cytosol supernatants. Autoradiographs are shown after SDS-gel electrophoresis. B, MRP1 recycling assay by biotin labeling the cell surface for 30 min, followed by pulse-chase periods for the times shown. MRP1 was immunoprecipitated by MRP1 antibody at various times, as described in "Materials and Methods."

microscopy, cell fractionation, and metabolic and cell surface labeling protocols, we conclude that MRP1 is accumulating in a cytosolic compartment through which MRP1 normally recycles (see Fig. 6B, biotinylation experiment). We have demonstrated that MRP1 is located in a lighter, lower-density fraction in the KB-CP.5 cells compared with its localization in the KB-3-1 cells. The specific vesicles in which MRP1 accumulates appear to be distinct from normal membrane components, in that they are less dense, and even after centrifugation at >100,000 × g, they remain in supernatant fractions. This compartment colocalizes with both a Golgi marker and, to some extent, with an ER marker, as shown in Fig. 4, and, hence, is part of the *trans*-Golgi network (16).

What is the defect in the cisplatin-resistant cells that results in the mislocalization of MRP1 and other plasma membrane proteins? Although much progress has been made in understanding the process by which cell surface components recycle, the nature of the recycling vesicles is unclear. Intracellular recycled caveolin is known to be present in *trans*-Golgi network vesicles in the cytosol (17), but there is still considerable debate about the role of caveolin in the recycling process. Caveolin appears to be increased in amount in the KB-CP cells (data not shown) as is the EEA1 marker of early endosomes (Fig. 5), but the significance of these observations is not known, unless these proteins are accumulating in the cells because of a block in recycling. Defects in lipid microdomains, or rafts (18, 19) in small G proteins, such as *ras*-related small GTP-binding protein 5 (Rab5), Ras-associated protein (Rap1), and/or ADP-ribosylation factor (Arf6; Refs. 20 and 21), or in the actin cytoskeleton (22, 23), could also be responsible for the defect observed in our cells. Recently, it has been shown that localization of certain membrane proteins in cells requires that the membrane proteins be anchored to the cytoskeleton (24). Thus, another possible defect in the KB-CP cells could be a failure to

anchor properly the membrane protein to the cytoskeleton, resulting in mislocalization or failure to remain in the plasma membrane.

The lysosomal defect seen in the KB-CP cells is manifested by reduced acidification in the single-step variants (the present study) and by a defect in processing by lysosomes of ligands internalized from the cell surface, such as EGF, in more highly resistant KB-CP cells, and decreased processing of lysosomal proteases (7). This defect may reflect, and possibly be the cause of, the defect in membrane vesicle recycling. Lysosomes are considered part of the *trans*-Golgi network of intracellular membranes (25, 26), and many cell surface proteins and ligands are delivered to lysosomes after internalization. The failure of lysosomal acidification could reflect a general defect in acidification of endosomes, which is essential for normal endocytosis. Maintenance of the appropriate pH in different subcellular compartments is essential to a variety of cell functions (14). Vesicular function and recycling are very sensitive to even small alterations in compartment pH, which can affect vesicular organization, endocytosis, and transport from the *trans*-Golgi complex to the plasma membrane. Defects in the pH of intracellular organelles are correlated with disruption in the function and organization of the *trans*-Golgi network and the pericentriolar recycling compartment (27).

The form of MRP1 accumulated in the cytoplasm of KB-CP cells appears to be less highly glycosylated than MRP1 from parental KB cells. This defect could reflect activity of deglycosylases in the cytosolic compartment in which MRP1 accumulates, incorrect trafficking of MRP1 through the Golgi as it goes to the cell surface, altered environment for activity of glycosylases, or altered localization of glycosylases in the resistant cells. The abnormalities we observe in

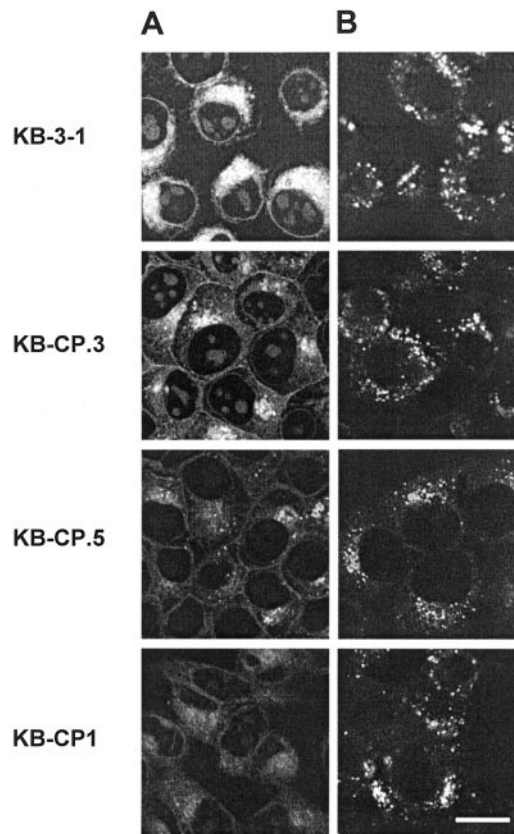


Fig. 7. Neutralization and morphology of lysosomes labeled with LysoSensor and LysoTracker. The following was as described in "Materials and Methods." Cells were labeled by LysoSensor green DND-189 (A), which is a pH-dependent probe, or labeled by LysoTracker red DND-99 (B). Reduced fluorescence intensity of lysosomes indicates neutralization of lysosomal pH. Scale bar, 10 μm.

MRP1 glycosylation could also be caused by the acidification defect because vacuolar pH regulates glycoprotein processing (28, 29).

In studies of highly cisplatin-resistant cell lines, we have found a general defect in uptake of many different molecules that normally enter cells by energy-dependent uptake or facilitated transport. The defect in these cells includes reduced uptake of glucose, reduced iron uptake via the transferrin receptor, and reduced uptake of amino acids (10). Cross-resistance to nucleoside analogues is presumed to be caused by reduced nucleoside transporters on the cell surface of KB-CP cells. Cross-resistance to heavy metals probably reflects the need for specific carriers; we have been able to demonstrate reduced arsenite and arsenate-binding proteins on the surface of KB-CP cells (1). Resistance to *Pseudomonas* enterotoxin, known to enter cells by receptor-mediated endocytosis, is also found in our most resistant KB-CP cells (7).

Several of the observations made in this study could have consequences for the use of cisplatin in the clinic. First, most cisplatin-resistant cell lines studied in the laboratory show reduced accumulation of cisplatin (30). Although this observation has not yet been confirmed in clinical specimens, it should be possible to collect the needed data. Second, the phenotype described here appears to be common in at least two different cell lines studied in the laboratory (an epidermoid adenocarcinoma and a hepatoma) and may be a common adaptation of cancer cells in patients for growth in cisplatin, because the frequency of these variants is quite high ($>1 \times 10^{-4}$). Third, it will be easy to detect protein mislocalization in clinical samples using histochemical techniques, thereby confirming the presence of the phenotype. Fourth, because proteins appear to be missing from the cell surface in the cisplatin-resistant cells, it should be possible, using existing imaging technology, to evaluate cancers in patients for this phenotype. Finally, understanding this mechanism of cisplatin resistance may aid in the design of new platinum analogues that enter cells by other means, or it may be possible to correct the trafficking defect in cisplatin-resistant cells once the mechanism of the defect is understood.

ACKNOWLEDGMENTS

We are grateful to Ira Pastan, Irwin Arias, and Chava Kimchi-Sarfaty for comments on the manuscript and to Joyce Sharrar and George Leiman for manuscript preparation.

REFERENCES

- Shen, D. W., Pastan, I., and Gottesman, M. M. Cross-resistance to methotrexate and metals in human cisplatin-resistant cell lines results from a pleiotropic defect in accumulation of these compounds associated with reduced plasma membrane binding proteins. *Cancer Res.*, **58**: 268–275, 1998.
- Chu, G. Cellular responses to cisplatin. The roles of DNA-binding proteins and DNA repair. *J. Biol. Chem.*, **269**: 787–790, 1994.
- Adachi, S., Obaya, A. J., Han, Z., Ramos-Desimone, N., Wyche, J. H., and Sedivy, J. M. c-Myc is necessary for DNA damage-induced apoptosis in the G(2) phase of the cell cycle. *Mol. Cell Biol.*, **21**: 4929–4937, 2001.
- Rong, R., He, Q., Liu, Y., Sheikh, M. S., and Huang, Y. TC21 mediates transformation and cell survival via activation of phosphatidylinositol 3-kinase/Akt and NF- κ B signaling pathway. *Oncogene*, **21**: 1062–1070, 2002.
- Shen, D. W., Cardarelli, C., Hwang, J., Cornwell, M., Richert, N., Ishii, S., Pastan, I., and Gottesman, M. M. Multiple drug-resistant human KB carcinoma cells independently selected for high-level resistance to colchicine, adriamycin, or vinblastine show changes in expression of specific proteins. *J. Biol. Chem.*, **261**: 7762–7770, 1986.
- Johnson, S. W., Shen, D., Pastan, I., Gottesman, M. M., and Hamilton, T. C. Cross-resistance, cisplatin accumulation, and platinum-DNA adduct formation and removal in cisplatin-sensitive and -resistant human hepatoma cell lines. *Exp. Cell Res.*, **226**: 133–139, 1996.
- Chauhan, S. S., Liang, X.-J., Su, A. W., Pai-Panandiker, A., Shen, D.-W., Hanover, J. A., and Gottesman, M. M. Reduced endocytosis and altered lysosome function in cisplatin resistant cell lines. *Br. J. Cancer*, **88**: 1327–1334, 2003.
- Ishikawa, T., Bao, T. T., Yamane, Y., Akimaru, K., Frindrich, K., Wright, C. D., and Kuo, M. T. Coordinated induction of MRP/GS-X pump and γ -glutamylcysteine synthetase by heavy metals in human leukemia cells. *J. Biol. Chem.*, **271**: 14981–14988, 1996.
- Sharp, S. Y., Smith, V., Hobbs, S., and Kelland, L. R. Lack of a role for MRP1 in platinum drug resistance in human ovarian cancer cell line. *Br. J. Cancer*, **78**: 175–180, 1998.
- Shen, D. W., Goldenberg, S., Pastan, I., and Gottesman, M. M. Decreased accumulation of [14 C]carboplatin in human cisplatin-resistant cells results from reduced energy-dependent uptake. *J. Cell. Physiol.*, **183**: 108–116, 2000.
- Akiyama, S., Fojo, A., Hanover, J. A., Pastan, I., and Gottesman, M. M. Isolation and genetic characterization of human KB cell lines resistant to multiple drugs. *Somatic Cell Mol. Genet.*, **11**: 117–126, 1985.
- Shen, D. W., Akiyama, S., Schoenlein, P., Pastan, I., and Gottesman, M. M. Characterisation of high-level cisplatin-resistant cell lines established from a human hepatoma cell line and human KB adenocarcinoma cells: cross-resistance and protein changes. *Br. J. Cancer*, **71**: 676–683, 1995.
- Suzaki, E., and Kataoka, K. Three-dimensional visualization of the Golgi apparatus: observation of Brunner's gland cells by a confocal laser scanning microscope. *J. Struct. Biol.*, **128**: 131–138, 1999.
- Mellman, I., Fuchs, R., and Helenius, A. Acidification of the endocytic and exocytic pathways. *Annu. Rev. Biochem.*, **55**: 663–700, 1986.
- Ishida, S., Lee, J., Thiele, D. J., and Herskowitz, I. Uptake of the anticancer drug cisplatin mediated by the copper transporter Ctr1 in yeast and mammals. *Proc. Natl. Acad. Sci. USA*, **99**: 14298–14302, 2002.
- Mellman, I., and Warren, G. The road taken: past and future foundations of membrane traffic. *Cell*, **100**: 99–112, 2000.
- Dupree, P., Parton, R. G., Raposo, G., Kurzchalia, T. V., and Simons, K. Caveolae and sorting in the trans-Golgi network of epithelial cells. *EMBO J.*, **12**: 1597–1605, 1993.
- McLauchlan, H. J., James, J., Lucocq, J. M., and Ponnambalam, S. Characterization and regulation of constitutive transport intermediates involved in trafficking from the trans-Golgi network. *Cell. Biol. Int.*, **25**: 705–713, 2001.
- Donaldson, J. G., and Lippincott-Schwartz, J. Sorting and signaling at the Golgi complex. *Cell*, **101**: 693–696, 2000.
- De Renzis, S., Sonnichsen, B., and Zerial, M. Divalent Rab effectors regulate the sub-compartment organization and sorting of early endosomes. *Nat. Cell Biol.*, **4**: 124–133, 2002.
- Brown, F. D., Rozelle, A. L., Yin, H. L., Balla, T., and Donaldson, J. G. Phosphatidylinositol 4,5-bisphosphate and Arf6-regulated membrane traffic. *J. Cell Biol.*, **154**: 1007–1017, 2001.
- Niles, W. D., and Malik, A. B. Endocytosis and exocytosis events regulate vesicle traffic in endothelial cells. *J. Membr. Biol.*, **167**: 85–101, 1999.
- Sheff, D. R., Kroschewski, R., and Mellman, I. Actin dependence of polarized receptor recycling in Madin-Darby canine kidney cell endosomes. *Mol. Biol. Cell*, **13**: 262–275, 2002.
- Apodaca, G. Endocytic traffic in polarized epithelial cells: role of the actin and microtubule cytoskeleton. *Traffic*, **2**: 149–159, 2001.
- Benjamin, S., and Glick, E. R. Export: more than one way out. *Curr. Biol.*, **11**: R361–R363, 2001.
- Traub, L. M., and Kornfeld, S. The trans-Golgi network: a late secretory sorting station. *Curr. Opin. Cell Biol.*, **9**: 527–533, 1997.
- Larsen, A. K., Escargueil, A. E., and Skladanowski, A. Resistance mechanisms associated with altered intracellular distribution of anticancer agents. *Pharmacol. Ther.*, **85**: 217–229, 2000.
- Welsh, M. J. Acidification indication. *Nature (Lond.)*, **352**: 23–24, 1991.
- Barasch, J., Kiss, B., Prince, A., Saiman, L., Gruenert, D., and al-Awqati, Q. Defective acidification of intracellular organelles in cystic fibrosis. *Nature (Lond.)*, **352**: 70–73, 1991.
- Niedner, H., Christen, R., Lin, X., Kondo, A., and Howell, S. B. Identification of genes that mediate sensitivity to cisplatin. *Mol. Pharmacol.*, **60**: 1153–1160, 2001.

Cancer Research

The Journal of Cancer Research (1916–1930) | The American Journal of Cancer (1931–1940)

Mislocalization of Membrane Proteins Associated with Multidrug Resistance in Cisplatin-resistant Cancer Cell Lines

Xing-Jie Liang, Ding-Wu Shen, Susan Garfield, et al.

Cancer Res 2003;63:5909-5916.

Updated version Access the most recent version of this article at:
<http://cancerres.aacrjournals.org/content/63/18/5909>

Cited articles This article cites 30 articles, 9 of which you can access for free at:
<http://cancerres.aacrjournals.org/content/63/18/5909.full#ref-list-1>

Citing articles This article has been cited by 18 HighWire-hosted articles. Access the articles at:
<http://cancerres.aacrjournals.org/content/63/18/5909.full#related-urls>

E-mail alerts [Sign up to receive free email-alerts](#) related to this article or journal.

Reprints and Subscriptions To order reprints of this article or to subscribe to the journal, contact the AACR Publications Department at pubs@aacr.org.

Permissions To request permission to re-use all or part of this article, use this link
<http://cancerres.aacrjournals.org/content/63/18/5909>.
Click on "Request Permissions" which will take you to the Copyright Clearance Center's (CCC) Rightslink site.